

Indirect laser sintering of corrugated flow field plates for direct methanol fuel cell applications

Kumaran M Chakravarthy and David L Bourell,

Materials Science and Engineering Program,

Laboratory of Freeform Fabrication, The University of Texas at Austin, Austin, TX-78712

Abstract

REVIEWED, August 17 2011

Direct methanol fuel cells (DMFC) hold distinct advantages over traditional hydrogen-based fuel cells. Their commercialization, however, has been bound by many factors – especially their sub-optimal efficiency. This work aims at enhancing the performance of DMFC through the use of corrugated flow field plates. Our objectives are two-fold – one, to increase the power density of DMFC by corrugating flow field plates and two, to introduce Laser sintering (LS) as an efficient and robust method for the manufacture of such plates. Corrugated flow field plates with 10% more surface area as compared to a planar design were made by LS & tested in a DMFC environment. Our results show that the particle size of the material used – Graphite – has a significant effect upon the green strength of LS parts. We also report the performance of corrugated flow field plates with 10% higher surface area (as compared to planar plates), channel width and depth of 2mm and an electrode area of 5 cm². This study is the first experimental approach to the use of indirect LS for making such fuel cell components.

1. Introduction

1.1 Non planar designs in fuel cells

Direct methanol fuel cells (DMFC) use liquid methanol as a fuel, which has higher energy density than hydrogen. In addition, methanol is cheap, easy to store and handle compared to hydrogen. All these present a unique advantage of DMFC over hydrogen based fuel cells. However commercialization of DMFC has been slow due to various issues including cost, complexity, low operating voltage and efficiency [1, 2]. Attempts are made to improve the performance of these DMFC [3]. One way of improving the performance of the fuel cells is by improving the power density. Power density of a fuel cell can be increased by increasing the surface area/volume ratio of the fuel cell. Increasing the surface area increases the reaction surface where methanol oxidation and or oxygen reduction takes place thereby enhances the performance of the fuel cell. Merida *et. al* [4] proposed a proton exchange membrane fuel cell [PEMFC] design with a non planar membrane electrode assembly (MEA) architecture that improved the volumetric power density. The waved tube cell (WTC) concept proposed has been prototyped with two designs- one where the waved MEA was supported by a ribbed graphite plates and the other with a waved MEA supported by waved expanded metallic structure. Significant gains in volumetric power density have been achieved using the WTC architecture. Li *et. al* [5] developed and tested a non planar- wave like PEMFC with undulated MEA and perforated bipolar plates. Gains in volumetric power density and specific power with the novel wave like architecture stacks were reported. Laam Tse [6] attempted to improve the power density of the DMFC by corrugating the membrane electrode assembly by pressing and folding methods. An analytical model was developed to analyze the relationship between area-to-volume ratio (A/V) and the corrugation aspect ratios. The model predicted a greater increase in A/V for

3-D corrugation. Experiments were done to validate the model and it was found that the overall power output was reduced. However since the projected surface area was reduced, the projected power density was increased for MEA corrugations with aspect ratios of 1.25. For MEA with aspect ratios 0.75, the performance was either identical or lower than the projected planar MEA. This performance degradation was attributed to the mechanical degradation introduced during the corrugation process. All the above work has either metallic current collector and/or ribbed graphite plates. Metallic bipolar plates have been known to corrode under the conditions seen in a fuel cell.

Bipolar plates made from graphite are highly desirable in fuel cell applications due to the properties of high electrical conductivity, low weight and resistance to corrosion that graphite possesses. However, the poor mechanical properties of natural graphite lead to prohibitive machining costs [7]. Indirect laser sintering (LS) provides an alternative way to manufacture bipolar plates using graphite-phenolic system [8]. The main advantage of the LS process is the design flexibility. Corrugated flow field plates, which are difficult to machine into a graphite block, may be made using the LS process and tested for their performance in a DMFC condition.

1.2 Green strength of laser sintered parts

The green strength of the graphite-phenolic composites made by LS is not good, 1-2 MPa [9]. Often parts break while trying to remove them from LS machine. This issue becomes complicated when using corrugated plates. So to improve the green strength, attempts were made by adding Nylon/11 [10] and carbon fiber [11]. Nylon/11 additions degraded the green strength and carbon fiber additions improved the green strength. The improvement in strength was offset by a dramatic drop in the electrical conductivity compared to a graphite-phenolic parts.

It becomes necessary to reassess the additions and their concentration. In addition, LS process parameters are optimized to observe if improvements in green strength can be obtained without adding new material to the graphite-phenolic system. The effect of graphite particle size and effect of fast cure phenolic resin on the green strength are explored.

2. Experimental

2.1 Laser sintering and post processing of corrugated flow field plates

Corrugated flow field plates with 10% higher surface area than flat plates were designed using Solidworks™. The channel width and depth were 2 mm and the electrode area was 5 cm². These plates were made in a DTM Sinterstation 2000 (™) using graphite (#4012, Asbury Graphite Mills, Inc)-phenolic resin (Durite AD 332A, Hexion inc) mix. The parameters used for laser sintering were as follows: fill laser power (22-24 W), outline laser power (4 W), laser scan spacing (0.0762 mm), powder layer thickness (0.1016 mm), partbed temperature (85°C) and feed bin temperature (40°C). The green plates were carbonized in a vacuum furnace at 1200°C for 1 hour to convert the phenolic resin to amorphous carbon (brown part). The brown parts were then infiltrated with cyanoacrylate resin to make the plates fluid impermeable. The infiltrated plates were polished to remove the excess surface cyanoacrylate resin. Corrugated flow field plates with 10% more surface area and 2 mm channel dimensions made by this process are shown in Figure 1 below:



Figure 1: Corrugated plates with 10% more surface area compared to a flat plate. The channel dimensions are 2 mm.

2.2 Fuel cell testing

The electrochemical performance of the DMFC with the corrugated flow field plates were tested in a single cell fixture with 850 e fuel cell test station supplied by Scribner associates inc. MEA used was a commercial one purchased from fuel cell store [membrane: Nafion™ 117, anode catalyst: Pt/Ru/C, cathode catalyst: Pt/C (4 mg/cm²)]. The performance of the plates was characterized as a function of clamping torque (65, 70, and 78 lb-in torque), reactant flow direction (counter and parallel flow) and reactant flow rate (oxygen: 0.2 and 0.3 L/min, methanol: 9, 10, and 13 mL/min) to identify optimum parameters from the corrugated plates.

For studying the effect of clamping torque, the reactant flow direction was counter flow, methanol flow rate was 9 mL/min, oxygen flow rate was 0.2 L/min. For studying the effect of methanol flow rate, the conditions for testing were as follows: clamping torque: 70 lb-in, reactant flow direction: counter flow; 1 M methanol, oxygen flow rate: 0.2 L/min. For studying the effect of oxygen flow rate, the test conditions were as follows: clamping torque: 70 lb-in, reactant flow direction: counter flow; 1 M methanol, methanol flow rate: 9 mL/min. Fuel cell temperature was kept constant at 65°C for all test conditions.

Commercial plates with 1 mm channel dimensions were tested under the following conditions: clamping torque: 65 lb-in, reactant flow direction: counter flow; 1 M methanol, methanol flow rate: 6 ml/min; oxygen flow rate: 0.2 L/min, fuel cell temperature: 65°C.

2.3 Laser sintering process optimization for improved green strength

2.3.1 Effect of graphite particle size

Two types of graphite particle sizes GS 150 E (~ 75 μ) and GS 75 E (~ 27 μ) obtained from Graftech international were mixed independently with phenolic resin milled to a particle size of ~ 15 μ (novalac based, Durite AD 332 A) obtained from Hexion inc. The mixes were then loaded into a laser sintering machine DTM Sinterstation 2000 and three point bend specimens (5 in X 0.5 in X 0.125 in) were made with different fill laser powers. The specimens were tested using a

5 kN Instron machine (model 3345). The span length was set at 50 mm and a displacement rate of 0.1 mm/min was used. Maximum flexural stress was reported as the flexural strength.

2.3.2 Effect of fast curing phenolic resin

Phenolic resin contains two parts- a novolac resin and a curing agent- hexa methylene tetra amine (HMTA). Two types of phenolic resins were used in this experiment- one supplied by Plenco as a fast cure resin and other was supplied by Hexion inc- Durite AD 332 A. The Durite resin has ~ 8% of HMTA. Novolac is yellow in color and HMTA is white in color. 8% HMTA Durite is yellow in color and is referred to “yellow” Durite in this work. The new fast cure resin procured from Plenco is white in color indicating higher amounts of HMTA in the mix. In addition, the fast cure resin has higher amounts of free phenol and water molecules which improve the cross linking properties. Another Durite obtained from Hexion has higher HMTA and is white in color. This resin is called “white” Durite.

GS 75 E (27 μ) graphite was mixed with “yellow” Durite and Plenco fast cure phenolic separately in a 70:30 ratio by weight, and three point bend specimens were made using the parameters described earlier. For the Plenco mix, the partbed (70° C) and feed bin temperatures (30° C) were reduced to prevent the powder mix from caking.

The “white” Durite and “yellow” Durite were mixed separately with Asbury Carbon graphite (# 4012) with a particle size of ~75 μ in a 65:35 ratio by weight and LS three point bend specimens were made using the parameters described before.

3. Results and Discussion

3.1 Fuel cell performance tests

3.1.1 Effect of clamping torque

The polarization (potential vs. current density) curve and the power density curve for different clamping torque are given in the Figures 2 and 3 below. The performance of the fuel cell with corrugated plates was inferior compared to a fuel cell with commercial plates. The limiting current density for a corrugated plate fuel cell was ~150 mA/cm², whereas the limiting current density of a fuel cell with commercial plate was >300 mA/cm². This is assumed to be due to the channel size effect. The commercial plates had a channel width of 1 mm and the number of passes was ~15 for a 5 cm² area, whereas the 2 mm channel corrugated plates had 7 passes for the reactants to flow through. This decreased electrochemical area might have offset any potential gain from corrugating the plates. The performance of the corrugated plate will be compared with a flat base line plate of same channel dimensions.

The 70 lb-in torque gave better performance than 65 and 78 lb-in torque at high current densities. For low torques, the contact resistance was higher and for higher clamping torques, the gas diffusion layer protruded into the channels, thereby blocking the flow of reactants through the channels. Radhakrishnan and Haridoss [12] studied the difference in structure and properties of different diffusion media and their effect on performance of PEMFC flow field design. They found carbon fiber cloth as a diffusion layer lacked rigidity compared to a carbon paper. Carbon fiber cloth exhibited 43-125% more intrusion compared to carbon paper media. The pressure drop for a 3 mm wide channel was also more with a GDL compared to a 1 mm and 2 mm wide channels. This increased pressure drop may be another reason for reduced performance.

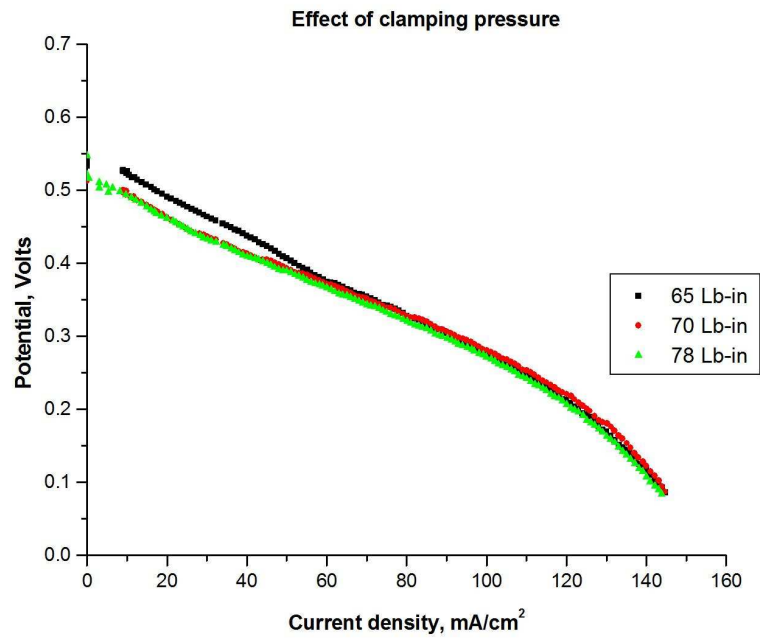


Figure 2: Effect of clamping torque on performance of DMFC with corrugated flow field plate (Figure 1), with a 7 pass, 2mm wide channel.

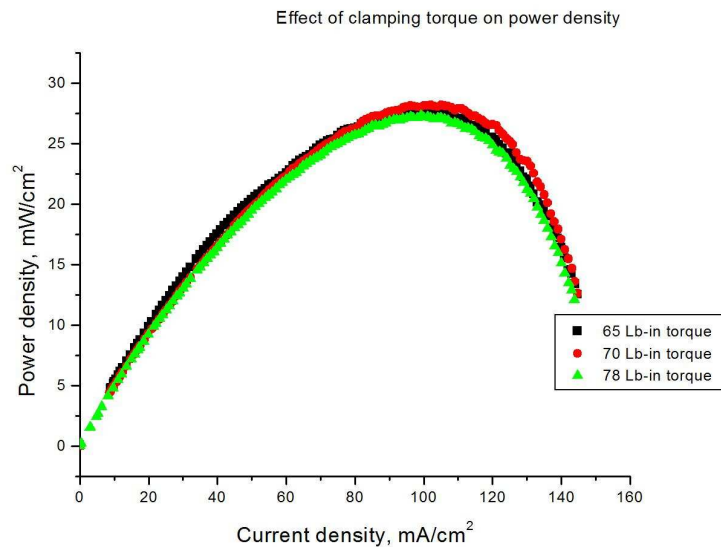


Figure 3: Effect of clamping torque on power density of DMFC with corrugated flow field plates (Figure 1). The performance is slightly better for moderate clamping torque (70 lb-in) at high current densities.

3.1.2 Effect of reactant flow direction- counter and parallel flow

Methanol solution and oxygen were made to flow in counter current and parallel direction to assess which of these two was favorable for a corrugated plate. From the Figures 4 and 5 below, it can be seen that parallel flow tends to show better performance in the high current region. This is contrary to the normal fuel cells where counter flow gives better performance.

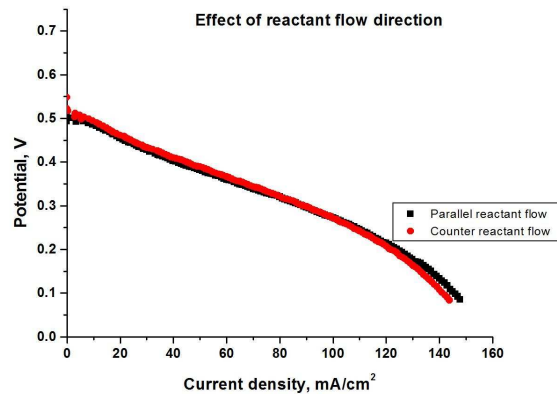


Figure 4: Polarization curve for DMFC as a function of reactant flow direction. The parallel flow tends to give better performance in the high current density region for corrugated bipolar plates.

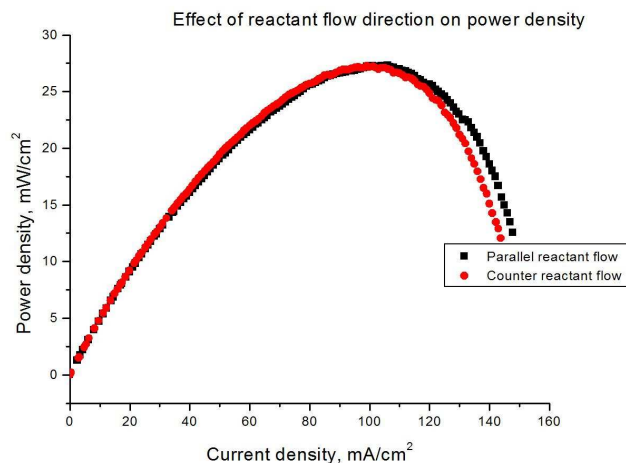


Figure 5: Effect of reactant flow direction: Parallel flow offers better performance than counter current flow for corrugated bipolar plates.

3.1.3 Effect of Methanol flow rate

Methanol flow rate had a significant effect on the polarization curve of fuel cell with corrugated flow field plates as seen in the Figure 6 and 7 below. Increasing the methanol flow rate from 9 mL/min to 13 mL/min degraded the performance in the high current region. At higher flow rate, the gas diffusion layer could be flooded leading to the poor performance.

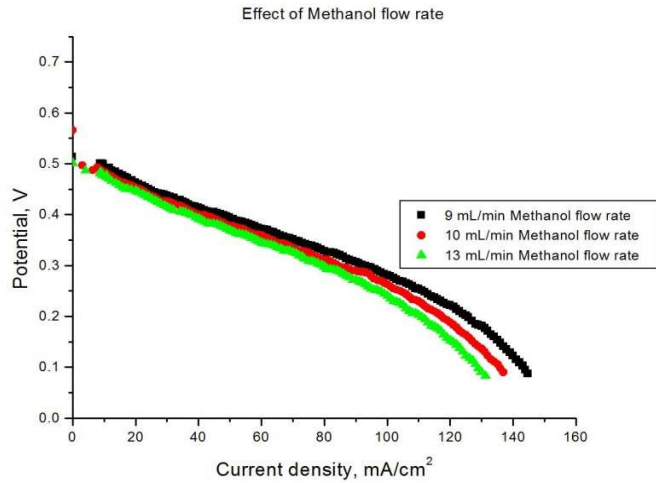


Figure 6: Effect of methanol flow rate on performance of DMFC with corrugated flow field plates. The performance decreases with higher methanol flow rate.

Figure 7 shows the power density curve for varying methanol flow rate. Oscillations seen in the curves may be from corrugated channels in the flow field plates. The peak power also shifted to lower current density with increasing flow rate.

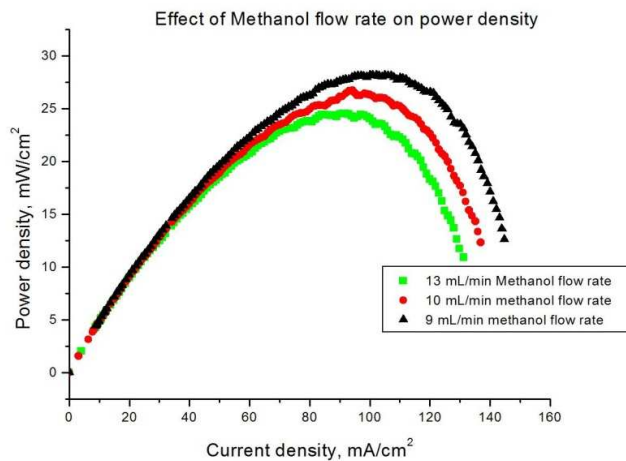


Figure 7: Effect of methanol flow rate on power density of DMFC with corrugated flow field plates. The power density decreases significantly with increasing the methanol flow rates. There are oscillations in the power density curves with increasing flow rates.

3.1.4 Effect of Oxygen flow rate

Increasing the oxygen flow rate from 0.2 L/min to 0.3 L/min degraded the performance of the fuel cell in high current region, Figures 8 and 9. Oscillations seen in both the polarization curve and power density curve could arise from corrugation in the flow channels. Also, the oscillations were more pronounced with higher flow rate, which was similar to the methanol flow rate experiments.

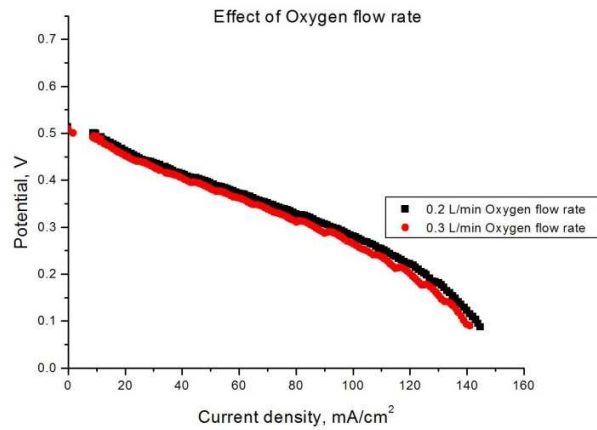


Figure 8: Effect of oxygen flow rate on performance of DMFC with corrugated flow field plates. Increasing the flow rate deteriorated slightly the performance in the high current region.

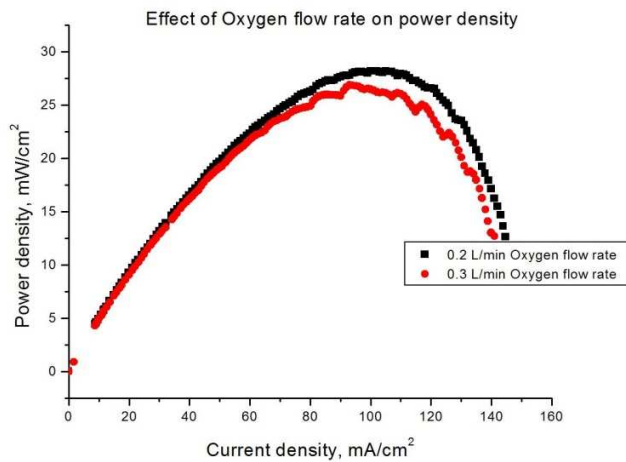


Figure 9: Effect of oxygen flow rate on the power density of DMFC with corrugated flow field plates. With a higher oxygen flow rate, the peak power decreased and shifted to left.

3.2 Laser sintering process optimization for increased green strength

3.2.1 Effect of graphite particle size

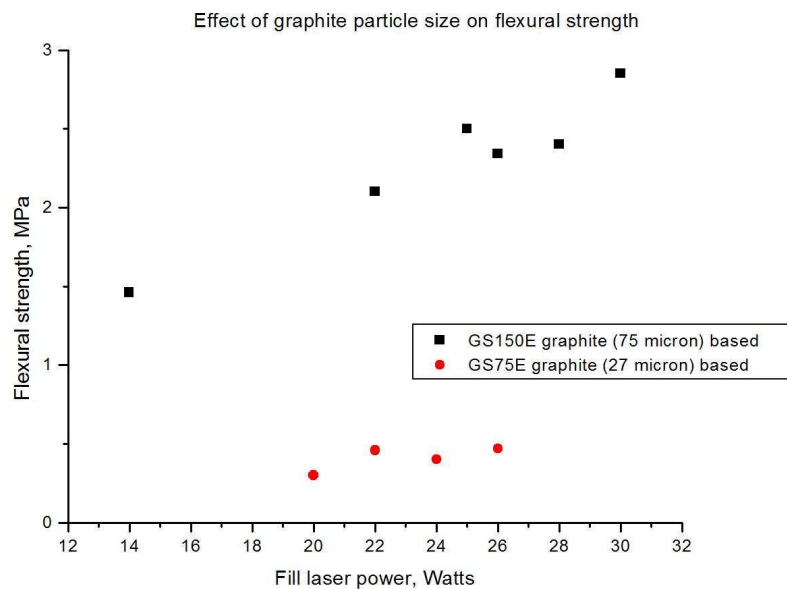


Figure 10: Effect of graphite particle size on green flexural strength of LS specimens. The graphite particle size significantly influenced the green flexural strength.

The green flexural strength was strongly influenced by the graphite particle size [Figure 10]. With a higher graphite particle size, the flexural strength was higher. This had been postulated to be due to the number of bridges formed by a finer phenolic resin around a large graphite particle which would be higher than that on a smaller graphite particle [8]. SEM micrographs for small graphite particle specimens [Figure 11a] show that the molten phenolic did not wet the graphite. Instead it re-solidified into fine globules. SEM micrographs of larger graphite specimens [Figure 11b] show that the phenolic resin was able to flow and wet the graphite particles. The BET surface area of 75 μ graphite was ~ 4 m²/g; while the surface area of 27 μ graphite was ~ 12 m²/g. Cross sectional SEM micrograph [Figure 12] shows that interlayer bonding is better for samples with large graphite particle size than samples with small graphite particles. This may be another reason for the difference in strength values. Also, the mix with large graphite particle size responded to laser power better than the mix with fine graphite size.

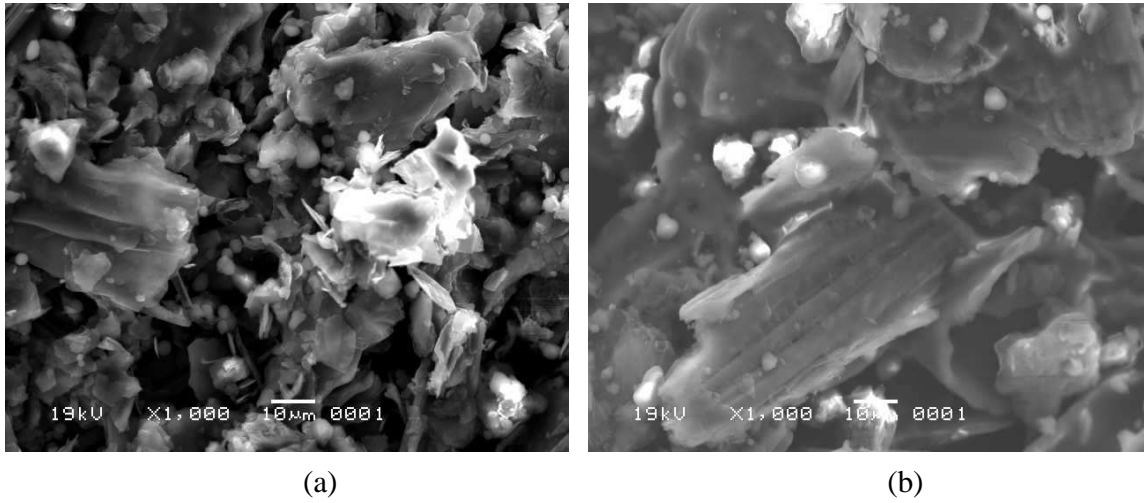


Figure 11: SEM micrographs (planar view) of a sample with 27 μ graphite (a) and sample with 75 μ (b) graphite. Note the phenolic is seen as small molten globules in (a) and is completely wetting graphite in (b). The BET surface area of the graphite particle is $\sim 12 \text{ m}^2/\text{g}$ (a) and $\sim 4 \text{ m}^2/\text{g}$ (b).

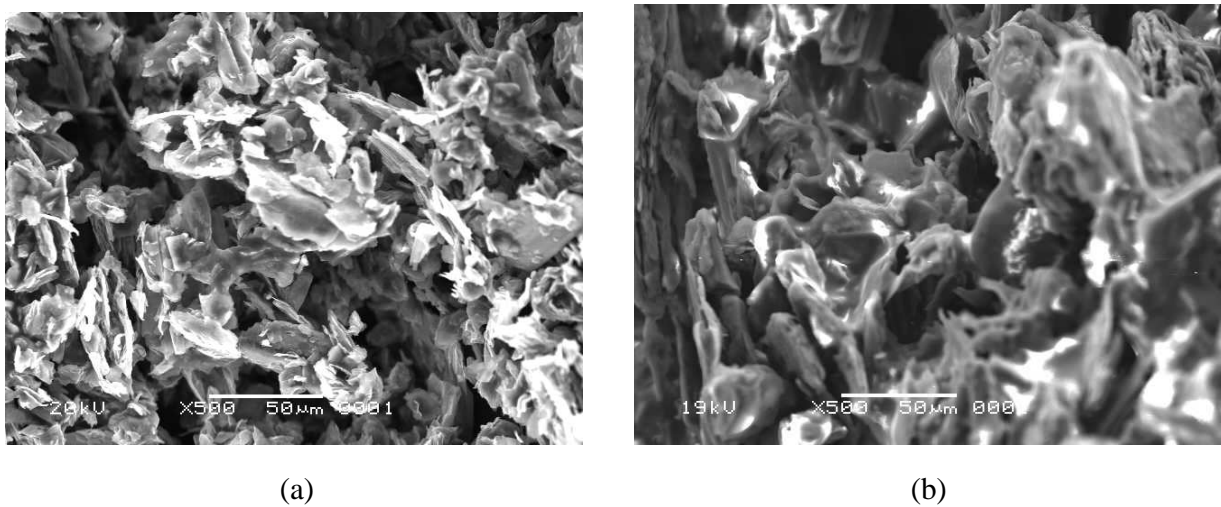


Figure 12: SEM micrographs (cross sectional view) of a sample with 27 μ graphite (a) and sample with 75 μ (b) graphite. Note the presence of large voids in (a) where as good interlayer bonding is seen in (b).

3.2.2 Effect of fast cure phenolic resin

(i) Plenco fast cure resin vs. yellow Durite

The Plenco fast cure resin when fed inside the laser sintering machine caked in the feed bins. This was attributed to the melting of free phenol in the resin and to prevent caking, temperature of the bins and partbed were lowered to 30° C and 75° C respectively. Parts made with those parameters yielded a flexural strength of $\sim 0.45 \text{ MPa}$, which was same as that of regular resin

[Figure 13]. This low value could also be due to the graphite particle size effect which might have reduced the influence of fast cure resin. SEM micrographs [Figures 14, 15] of samples made with both resin mixes showed similar features.

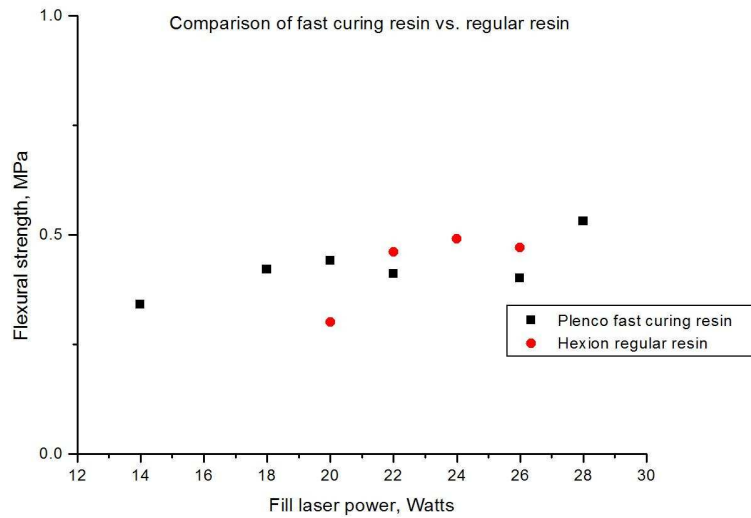
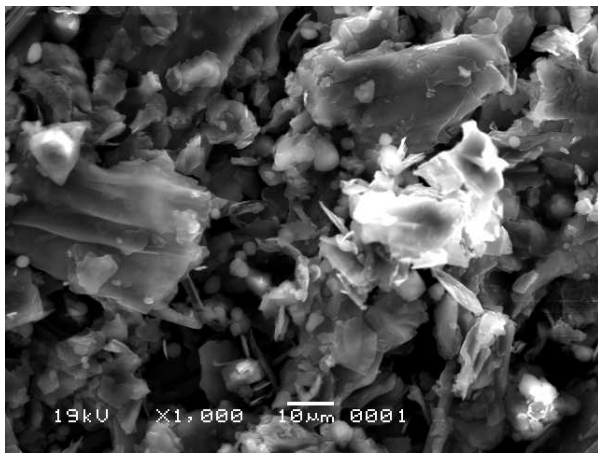
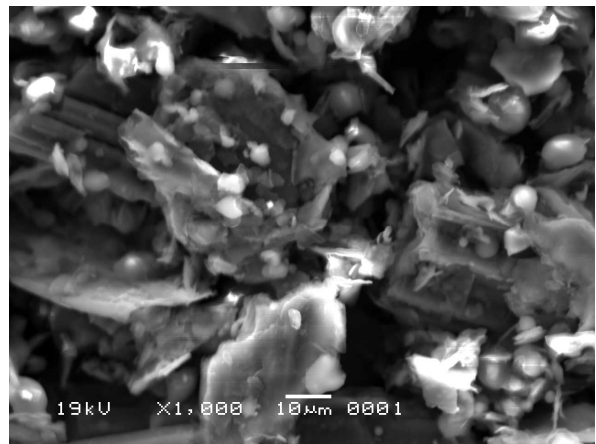


Figure 13: Effect of fast cure resin on green flexural strength of LS specimens. Graphite particle size was $\sim 27\mu$.



(a)



(b)

Figure 14: SEM micrographs (planar view) of a sample with yellow Durite (a) and sample with Plenco fast cure resin (b). The graphite particle size was 27μ graphite. Both the micrographs look similar with non-wetting fine phenolic molten globules. The strength values were also similar (~ 0.45 MPa).

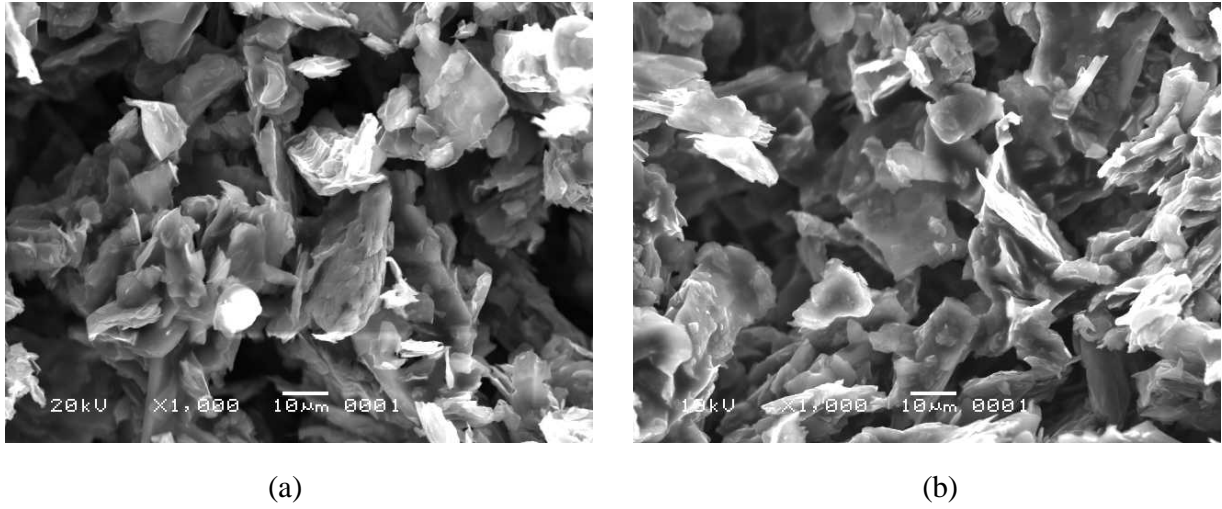


Figure 15: Cross sectional SEM micrographs of a sample with yellow Durite (a) and sample with Plenco fast cure resin (b). The graphite particle size was 27μ graphite. Both the micrographs look similar with large porosity. The strength values were also similar (~ 0.45 MPa).

(ii) White Durite vs. yellow Durite

The mix with 35 wt% white Durite gave strength levels ~ 3.5 - 3.75 MPa. This strength level was comparable to those achieved with up to 25 wt% carbon fiber additions [13]. The fill laser power seemed to have less effect on this composition. All the white Durite specimens made with 20-30 watts gave similar strength values [Figure 16]. The SEM micrograph of a white Durite specimen (Figure 17b) appears to be denser than the yellow Durite specimen (Figure 17a). A higher level of Hexamine in the white Durite resin leads to more densification than the yellow Durite resin. The mix with 35 wt% yellow Durite had slightly lesser strength levels (2.75- 3.5 MPa) and the difference was more pronounced when processed at lower energy levels. Yellow Durite as a resin is responsive to the laser power. The improvement achieved with white Durite over yellow Durite was comparable to the order of the strength of finer graphite mix (~ 0.4 MPa).

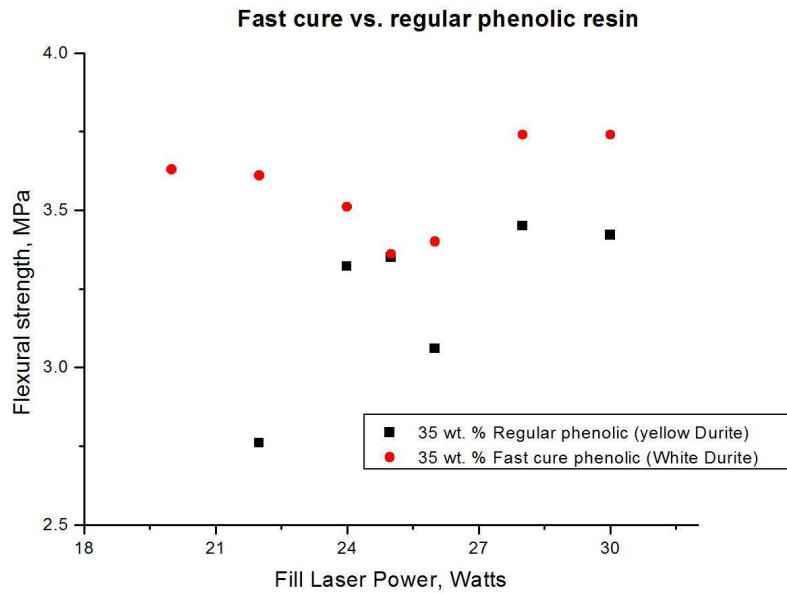


Figure 16: Effect of fast cure phenolic resin on the green flexural strength of LS specimens.

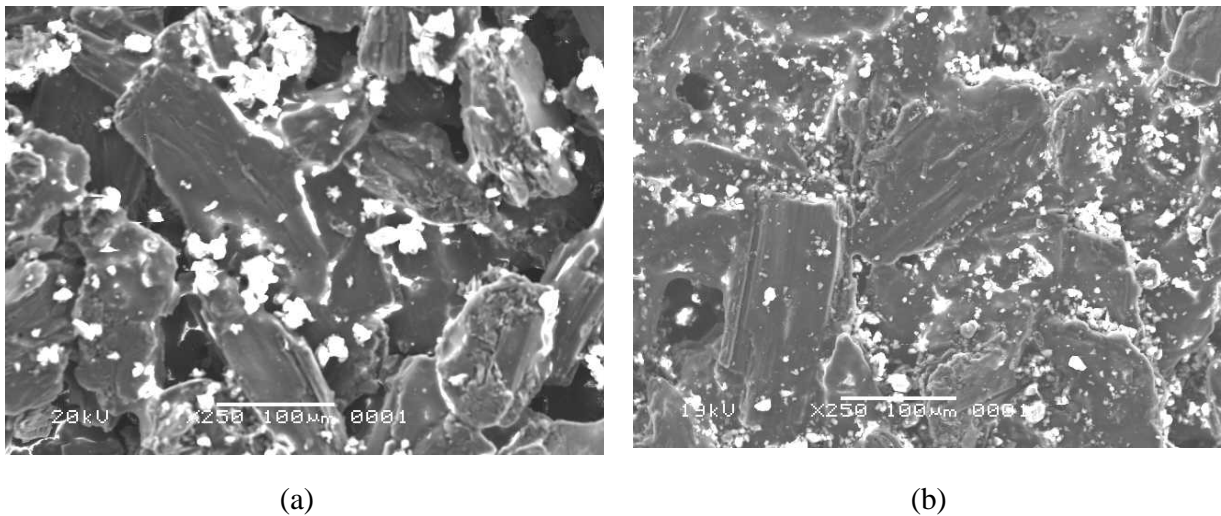


Figure 17: SEM micrographs (planar view) of 35wt% yellow Durite (a) and 35wt% white Durite (b) specimens. White Durite specimen is denser than the yellow Durite specimen.

The advantage of these mixes over the carbon fiber additions was the electrical conductivity of the brown/finished part would be higher because phenolic would change into conducting amorphous carbon after burnout. The electrical conductivity of specimens with 25 wt% carbon fiber was ~ 80 S/cm [11], which was lesser than the DOE requirement, 100 S/cm [14].

4. Conclusions and Future work

1. A corrugated flow field plate design with 10% more surface area compared to a planar design was made and tested for its performance in a fuel cell. New designs with higher corrugations and channel dimensions comparable to the commercial plates will be made and tested for their performance.
2. The green strength of the laser sintered parts was optimized by studying the effect of graphite particle size, fast cure phenolic resin and changing the composition of the mix. Graphite particle size had a significant effect on the green strength and larger particle sizes are preferred for higher green strength.
3. Two types of fast cure phenolic resin were tried. One resin (Plenco) was difficult to process inside the laser sintering machine due to caking. The laser sintering process parameters were modified significantly to enable the resin to be processed. The mix with higher HMTA (white Durite) resin in a 35: 65 (phenolic: graphite) ratio gave strength level comparable to a mix with 25 wt% of carbon fiber addition.

Acknowledgement

This work was supported by the Office of Naval Research MURI grant no. N00014-07-1- 0758. The authors thank the support of Mr. Albert V. Tamashauskyy of Asbury Graphite Mills, Inc. for discussions and help with supplying graphite used in this work. We are also grateful to Dr. Rajan Srinivasacharya and Mr. William Handel of Hexion specialty Chemicals Inc, Louisville, KY for discussions and for supplying phenolic resin used in this work. We are also grateful to Dr. Andreas Henke of Plastic Engineering Company, Sheboygan, WI for discussions and for supplying phenolic resin used in this work.

References

1. R. O'Hayre, S-W Cha, W. Colella, F. B. Prinz, John Wiley and Sons Inc., *Fuel cell fundamentals*, 2nd edition, 2009.
2. M. M. Mench, John Wiley and Sons Inc. "*Fuel cell engines*", 2008.
3. <http://www.me.utexas.edu/~dmfc-muri/>
4. W.R.Merida, G. McLean and N. Dijilali, "Non planar architecture for proton exchange membrane fuel cells", *Journal of Power Sources* 4452 (2001) 1-8
5. P.Y. Li, L.F. Peng, X.M. Lai, D.A. Liu and J. Ni, "A Novel Design of Wave-Like PEMFC stack with Undulate MEAs and Perforated Bipolar Plates", *Fuel Cells* 10 (2010) 111-117
6. L. A. Tse, "Membrane Electrode Assembly (MEA) design for power density enhancement of direct methanol fuel cells (DMFC)", *PhD Dissertation*, Georgia Institute of Technology, 2006.
7. G. O. Mepsted and J.M. Moore, Performance and Durability of Bipolar Plate Materials, *Handbook of fuel cells – Fundamentals, Technology and applications*, John Wiley and Sons Ltd., Vol. 3, pp.286-293, 2003.
8. S. Chen, "Fabrication of PEM Fuel Cell bipolar plate by Indirect selective laser sintering", *PhD dissertation*, The University of Texas at Austin, 2006.

9. K. Alayavalli and D.L. Bourell, "Fabrication of modified graphite bipolar plates by indirect selective laser sintering (SLS) for direct methanol fuel cells", *Rapid prototyping journal* 16(2010) 268-274
10. K.Chakravarthy and D.L. Bourell, "Binder development for indirect SLS of non-metallics", in the *Proceedings of Twenty First International Solid Freeform Fabrication Symposium*, Bourell et al., eds, pp 468-481, August 2010.
11. K. Alayavalli and D.L. Bourell, "Fabrication and Testing of Graphite Bipolar Plates for Direct Methanol Fuel Cells", in the *Proceedings of Twenty First International Solid Freeform Fabrication Symposium*, Bourell et al., eds, pp 468-481, August 2010.
12. V Radhakrishnan and P Haridos, "Differences in structure and property of carbon paper and carbon cloth diffusion media and their impact on proton exchange membrane fuel cell flow field design" *Materials and Design* 32 (2011) 861–868
13. D.L Bourell, M.C. Leu, K. Chakravarthy, N. Guo, K. Alayavalli, "Graphite-based indirect laser sintered fuel cell bipolar plates containing carbon fiber additions", *CIRP Annals - Manufacturing Technology* 60 (2011) 275–278
14. B.D. Cunningham and D. G. Baird, "Development of Bipolar Plates for Fuel Cells from Graphite Filled Wet-Lay Material and a Compatible Thermoplastic Laminate Skin Layer." *Journal of Power Sources* 168 (2007): 418-425.